

第十二届全国脉冲星研讨会 (2023)

# Hyperon star and hyperon-nucleon interaction research base on astronomical observation

Xiang-Dong Sun (孙向东)

Collaborators: Zhi-Qiang Miao (缪志强)

Bao-Yuan Sun (孙保元)

Ang Li (李昂)



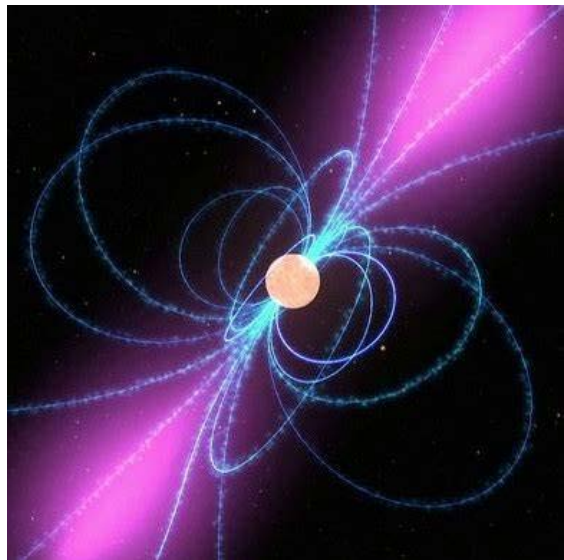
arXiv:2205.10631 ApJ

# Outline

- **Background & motivation**
- **Theoretical framework**
- **Bayesian analysis**
- **Discussion**
- **Summary**



# Background



- 1932 Landau et al. proposed the existence of neutron stars

- 1967 Bell et al. discovered the first neutron star

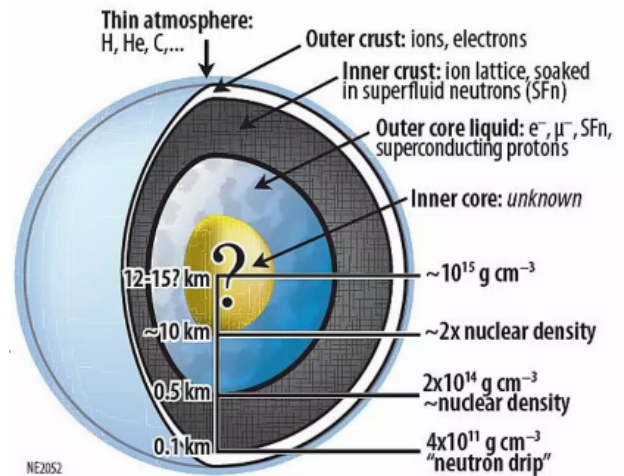


(image credit: NASA, NICER Team)



- GW170817 opens the era of GW multi-messenger astronomy

- Inner composition?



# Background

- Inner core component:  $\Lambda$  、  $\Sigma$  、  $\Xi$  、  $\Delta$ 、  $\Omega$ ...



LHC(EUR)



JLab(US)



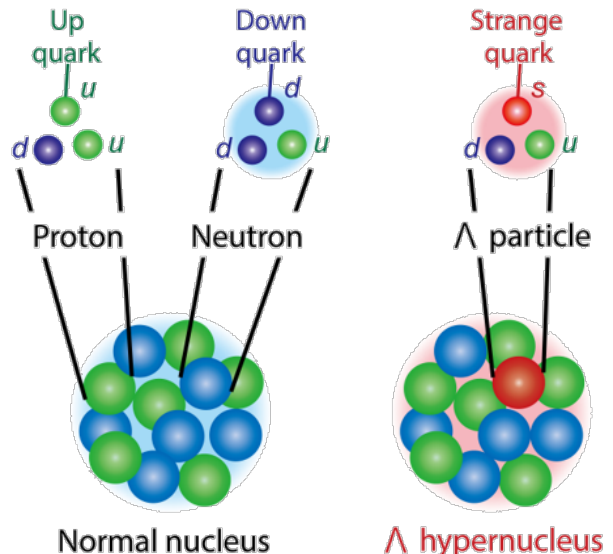
J-PARC(JPN)



FAIR(GER)



HIAF(CHN)



- Laboratory experiments: Extracting baryon–baryon interactions from hyperon–nucleon scattering, structure of the hypernucleus and reactions, ( half-life period  $\sim 10^{-10}$ s)
- Some available experimental data for single  $\Lambda$  separation energy

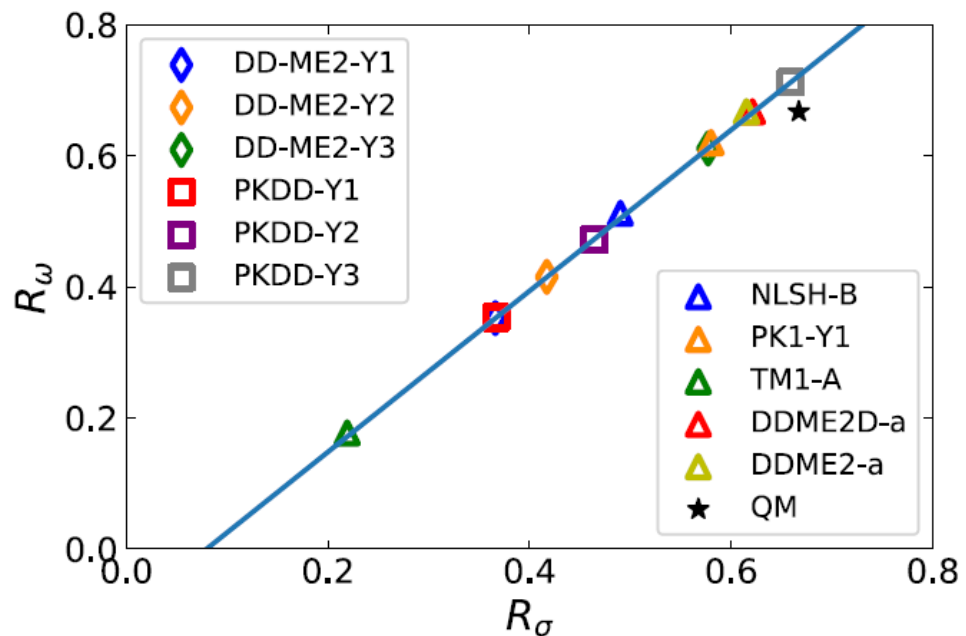
- The inner core of neutron stars might contain hyperons - **Hyperon stars**
- Difficulty : **Hyperon-nucleon interaction**, Model dependent.



# Motivation

Meson-hyperon coupling constant:  $g_{mY}$   
 Meson-nucleon coupling constant:  $g_{mN}$

$$R_{mY} = g_{mY}/g_{mN} \quad (m = \sigma, \omega, \rho, \delta)$$



Y. T. Rong et al. 2021 PRC  
 X. S. Wang et al. 2013 CTP  
 C. M. Keil et al. 2000 PRC

Rong et al PHYSICAL REVIEW C 104, 054321 (2021)

➤ Motivation: To combine the NICER mass, radii data of pulsars as well as GW170817 data and the strong correlation between hyperon nucleon interaction (Rong et al.), to perform Bayesian analysis to  $\Lambda$  hyperon nucleon interaction, and to constrain  $\Lambda$  hyperon nucleon interaction parameter space as well as the properties of hyperon stars.



## Theoretical model

➤ Model: Relativistic Mean Field (Baryon octet)

$$\mathcal{L}_{\text{free}}^B = \sum_B \bar{\psi}_B [i\gamma_\mu \partial^\mu - m_B] \psi_B;$$

$$\mathcal{L}_{\text{int}}^B = \sum_B \bar{\psi}_B [-g_{\sigma B} \sigma - g_{\omega B} \gamma_\mu \omega^\mu - g_{\rho B} \gamma_\mu \vec{\rho}^\mu \cdot \vec{\tau}] \psi_B;$$

$$\begin{aligned} \mathcal{L}_m = & -\frac{1}{2} m_\sigma^2 \sigma^2 + \frac{1}{2} m_\omega^2 \omega_\mu \omega^\mu + \frac{1}{2} m_\rho^2 \vec{\rho}_\mu \cdot \vec{\rho}^\mu \\ & + \frac{1}{2} \partial_\mu \sigma \partial^\mu \sigma - \frac{1}{4} \Omega_{\mu\nu} \Omega^{\mu\nu} - \frac{1}{4} \vec{R}_{\mu\nu} \cdot \vec{R}^{\mu\nu}; \end{aligned}$$

$$\begin{aligned} \mathcal{L}_{\text{NL}} = & -\frac{1}{3} g_2 \sigma^3 - \frac{1}{4} g_3 \sigma^4 + \frac{1}{4} c_3 (\omega_\mu \omega^\mu)^2 \\ & + \Lambda_v (g_{\omega B}^2 \omega_\mu \omega^\mu) (g_{\rho B}^2 \rho_\mu \rho^\mu); \end{aligned}$$

$$\begin{aligned} \mathcal{L}_{\text{4f}}^B = & -\frac{1}{2} \sum_B \alpha_S^{NB}(\rho) (\bar{\psi}_N \psi_N) (\bar{\psi}_B \psi_B) \\ & - \frac{1}{2} \sum_B \alpha_V^{NB}(\rho) (\bar{\psi}_N \gamma_\nu \psi_N) (\bar{\psi}_B \gamma_\nu \psi_B) \\ & - \frac{1}{2} \sum_B \alpha_{TS}^{NB}(\rho) (\bar{\psi}_N \vec{\tau} \psi_N) (\bar{\psi}_B \vec{\tau} \psi_B) \\ & - \frac{1}{2} \sum_B \alpha_{TV}^{NB}(\rho) (\bar{\psi}_N \vec{\tau} \gamma_\nu \psi_N) (\bar{\psi}_B \vec{\tau} \gamma_\nu \psi_B); \end{aligned}$$

$$\begin{aligned} \mathcal{L}_{\text{hot}}^B = & -\frac{1}{3} \beta_S^{NN} (\bar{\psi}_N \psi_N)^3 - \frac{1}{4} \gamma_S^{NN} (\bar{\psi}_N \psi_N)^4 \\ & - \frac{1}{4} \gamma_V^{NN} [(\bar{\psi}_N \gamma_\mu \psi_N)] [(\bar{\psi}_N \gamma^\mu \psi_N)]^2, \end{aligned}$$

➤ Nucleon-nucleon interaction:

17 effective RMF interactions:  
Walecka、DDRMF、NLRMF、DD-PC、NL-PC

➤ hyperon-nucleon interaction:

$R_{\sigma \Lambda}$   $R_{\omega \Lambda}$ : Relax SU(3) symmetry, [0 – 1]

$R_{\sigma \Sigma}$ ,  $R_{\omega \Sigma}$ ,  $R_{\rho \Sigma}$ ,  $R_{\sigma \Xi}$ ,  $R_{\omega \Xi}$ ,  $R_{\rho \Xi}$ :

- ✓ Vector coupling: SU(3) symmetry
- ✓ Scalar coupling: Potential depth

$$U_\Sigma = +34 \text{ MeV}$$

$$U_\Xi = -14 \text{ MeV}$$

$$\begin{aligned} R_{\sigma\Sigma} &= 0.443 & \text{Fortin et al. 2017 PRC;} \\ R_{\sigma\Xi} &= 0.302 & \text{Colucci \& Sedrakian 2013 PLB} \end{aligned}$$



## Bayesian Formula

- software: Python Bilby, PyMultiNest, Toast, Corner

$$P(\theta|D) = \frac{P(D|\theta)P(\theta)}{\int P(D|\theta)P(\theta)d\theta}$$

$P(\theta)$  is the prior probability of the parameter set  $\theta$

$P(D|\theta)$  is total likelihood function

$P(\theta)$	$R_{\sigma\Lambda} \sim U[0, 1]$ $R_{\omega\Lambda} \sim U[0, 1]$ . <span style="color: red;">NUCL</span>
	$\varepsilon_c \sim U[0.6 \times 10^{15}, 3 \times 10^{15}] \text{ g/cm}^3$ . $\varepsilon_c \sim U[0.3 \times 10^{15}, 1 \times 10^{15}] \text{ g/cm}^3$ <span style="color: red;">NICER</span> <span style="color: red;">PSR J0740+6620</span> <span style="color: red;">PSR J0030+0451</span>
	$\mathcal{M} \sim U[1.18, 1.21] M_\odot$ . $q \sim U[0.5, 1]$ <span style="color: red;">GW170817</span>



## Bayesian Formula

➤ **NICER**: PSR J0740+6620 and PSR J0030+0451

$$P_{\text{NICER}}(d_{\text{NICER}}|\theta) = \prod_j P_j(M(\theta), R(\theta))$$

Abbott et al. 2017 PRL  
Abbott et al. 2019 PRX

we equate the individual likelihood  $P_j$  to the joint posterior density distribution of  $M$  and  $R$

➤ **GW170817**:

$$P_{\text{GW}}(d_{\text{GW}}|\theta) = F(\Lambda_1(\theta; M_1), \Lambda_2(\theta; M_2), \mathcal{M}, q)$$

Abbott et al. 2017 PRL  
Abbott et al. 2019 PRX  
Hernandez et al. 2019 MN

$F(\cdot)$  is the interpolation function

$M_1$  and  $M_2$  are related to the chirp mass  $\mathcal{M}$  and the mass ratio  $q = M_2/M_1$

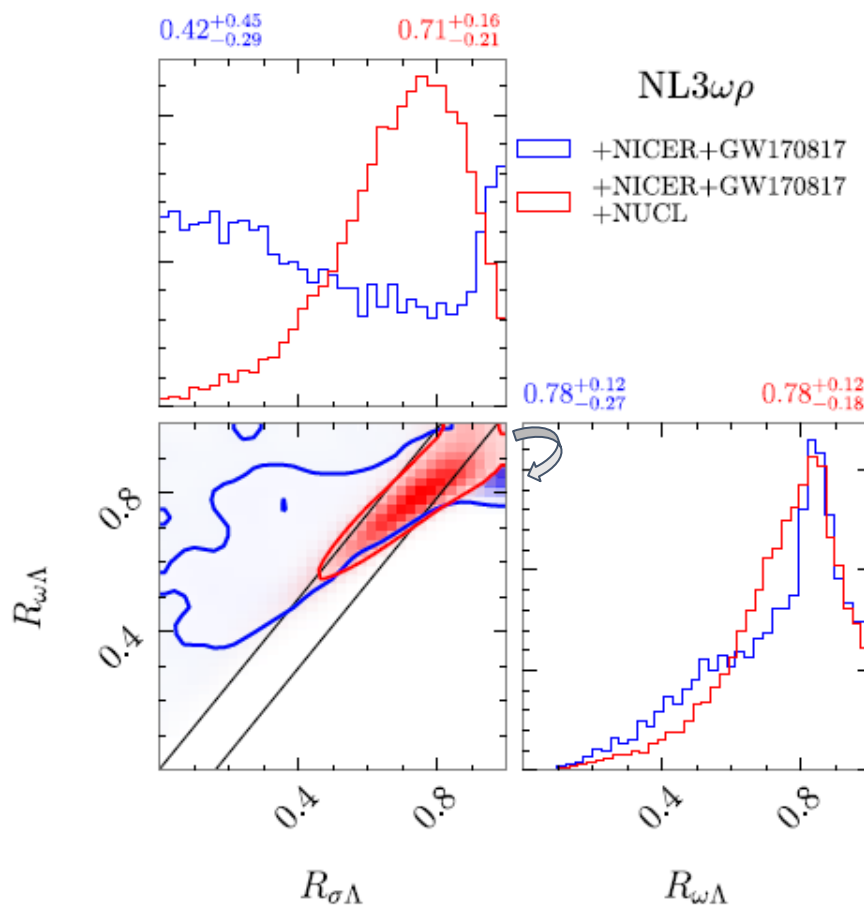
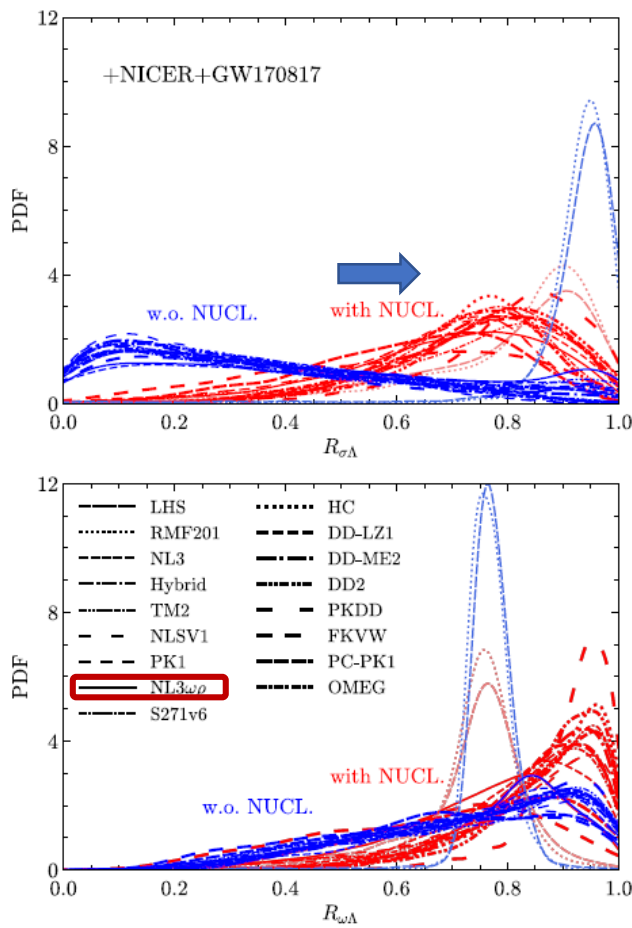
➤ **NUCL**: Single  $\wedge$  separation energy constraint

$$P_{\text{NUCL}}(d_{\text{NUCL}}|\theta) = \exp \left[ -\frac{1}{2} \frac{(R_{\sigma\Lambda} - \bar{R}_{\sigma\Lambda})^2}{\sigma_{R_{\sigma\Lambda}}^2} \right]$$

Rong et al. 2021 PRC



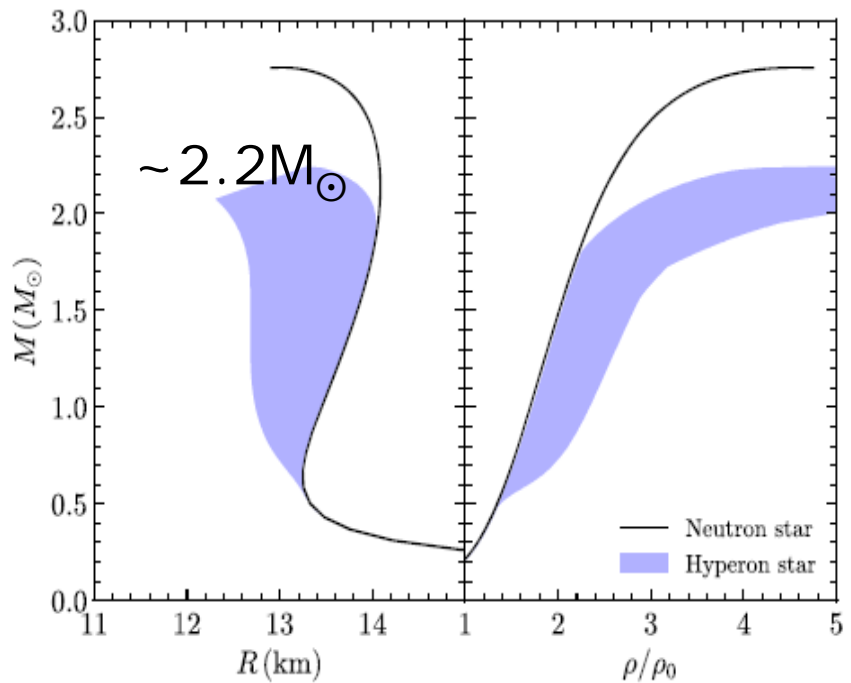
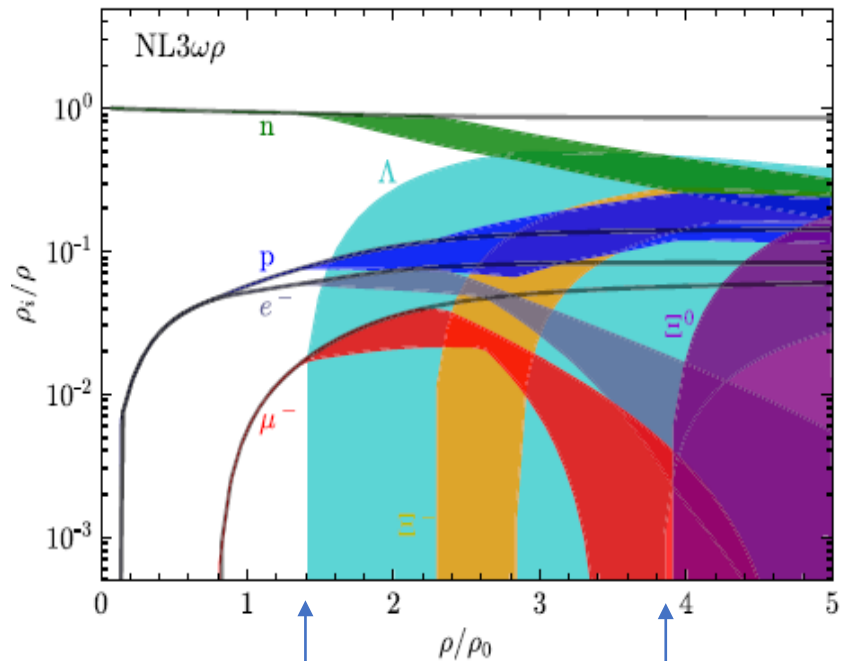
# $\Lambda$ hyperon-nucleon interaction



- Hypernuclei constraint **favors large values of  $R_{\sigma\Lambda}$  and  $R_{\omega\Lambda}$**  and disfavors small values of both couplings
- The addition of astrophysical observational data on top of the laboratory  $R_{\sigma\Lambda}$ - $R_{\omega\Lambda}$  correlation **rotates the linear correlation slightly** towards the direction of small values of  $R_{\omega\Lambda}$



## Properties of hyperon stars

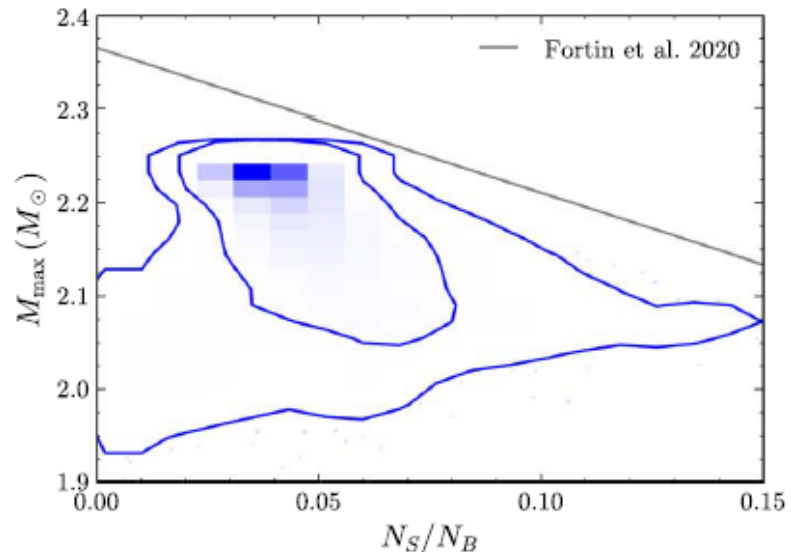
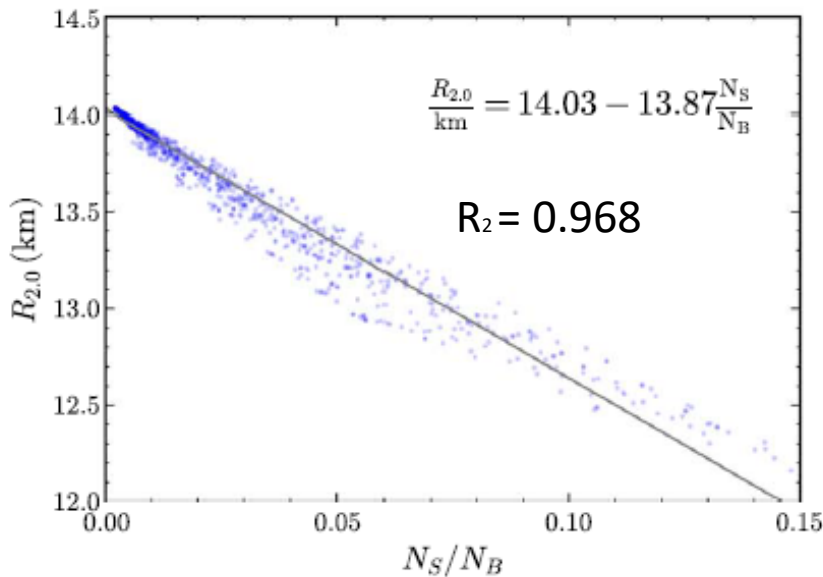
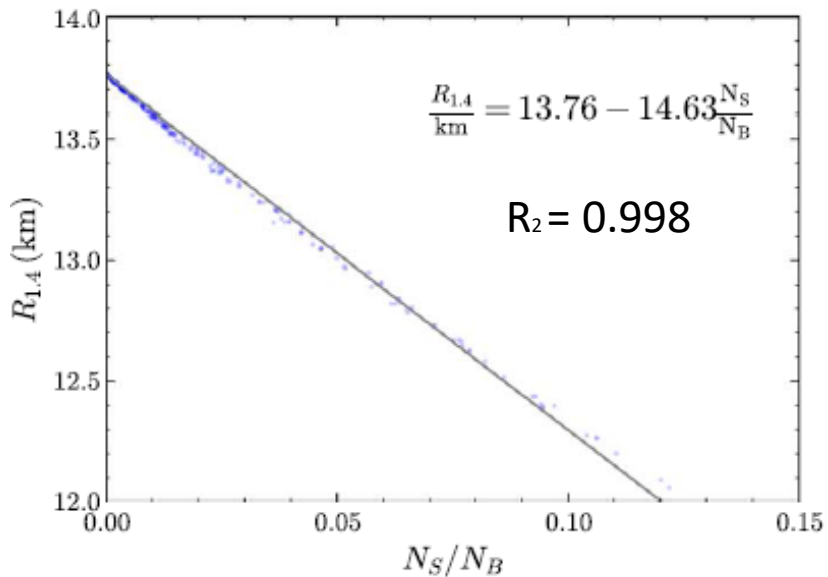


**Due to hyperons, the maximum mass is lowered by  $\sim 20\%$ :  $M_{\max} = 2.176^{+0.085}_{-0.202} M_\odot$  (68% credible interval).**

**From the referee** “The present article **addresses a long-standing issue** in neutron star physics, namely the hyperon puzzle. The authors **incorporate new information from hypernuclei calculations** and treat the hyperon couplings in a more general way than what exists in the present literature. This is an **interesting work that can have important future implications.**”



## Strangeness abundance



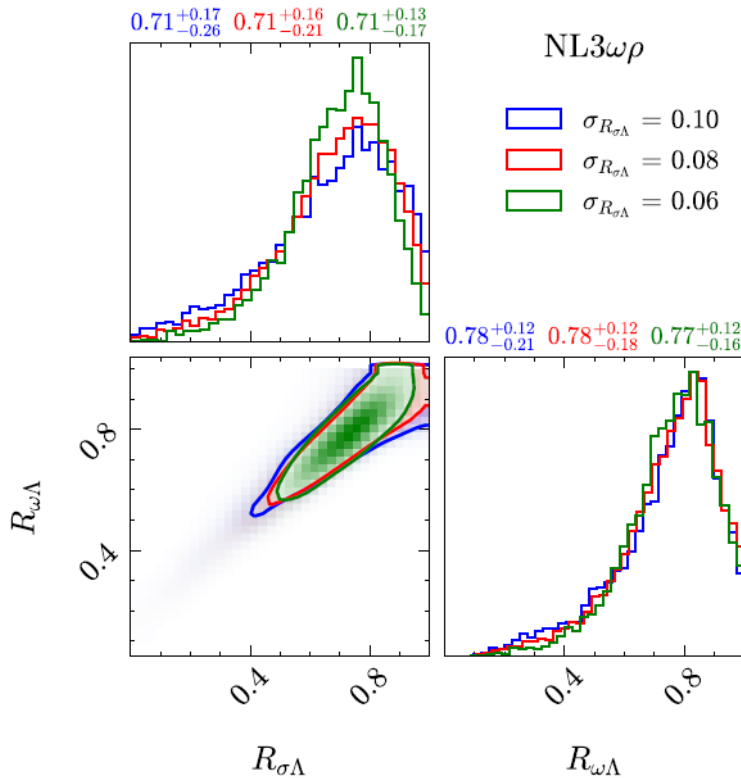
- Excellent **linear anticorrelations** between  $N_S/N_B$  and  $R_{1.4}$  as well as  $R_{2.0}$ , with the determination coefficients of  $R_2 = 0.998$  and  $R_2 = 0.968$ .
- There appears also an anticorrelation between  $N_S/N_B$  and  $M_{\text{max}}$  of hyperon stars.



## Summary

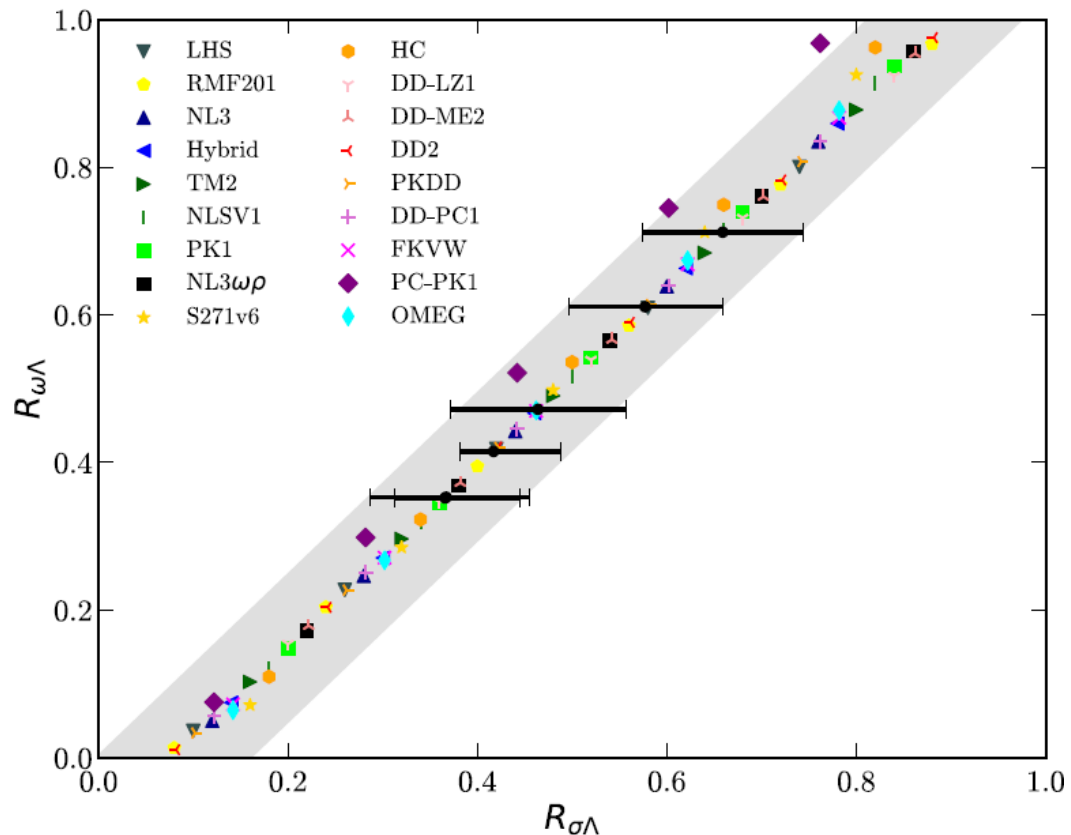
- We combine the **NICER &GW170817** data and the **strong correlations** of  $\Lambda$  hyperon-nucleon interactions to perform the Bayesian analysis with 17RMF models.
- We focus  $\Lambda$  hyperon, we **relax the SU(3) symmetry**, take accurately measured mass, radius (for PSR J0030+0451 and PSR J0740+6620), and tidal deformability (for GW170817) and laboratory constraint from the single  $\Lambda$  hypernuclei data.
- The laboratory constraint from the single  $\Lambda$  hypernuclei data determines the phenomenological interactions, **preventing a small R scalar coupling** through a strong positive correlation between the scalar and vector ones.
- We find the  $\Lambda$  hyperon **threshold can be as low as  $\sim 1.4$  times** the nuclear saturation density, and the hyperon star EOS is moderately stiff( **$M_{\max}=2.2M_{\odot}$** ).
- The decrease of the radii of typical  $1.4 M_{\odot}$  and  $2.0 M_{\odot}$  stars can both **be linearly depicted as functions of the strangeness fraction** in hyperon stars.

# Appendix



	$R_{\sigma\Lambda}$	$R_{\omega\Lambda}$	$M_{\max}/M_{\odot}$	$\rho_c/\rho_0$	$R_{2.0}/\text{km}$	$R_{1.4}/\text{km}$	$\Lambda_{1.4}$
$\sigma_{R_{\sigma\Lambda}} = 0.10$	$0.707^{+0.174}_{-0.261}$	$0.777^{+0.116}_{-0.209}$	$2.180^{+0.062}_{-0.228}$	$4.865^{+0.055}_{-0.565}$	$13.980^{+0.088}_{-1.533}$	$13.769^{+0.000}_{-1.086}$	$940.165^{+0.000}_{-448.040}$
$\sigma_{R_{\sigma\Lambda}} = 0.08$	$0.712^{+0.157}_{-0.215}$	$0.778^{+0.121}_{-0.183}$	$2.176^{+0.085}_{-0.202}$	$4.846^{+0.046}_{-0.501}$	$13.968^{+0.096}_{-1.512}$	$13.769^{+0.000}_{-1.084}$	$940.165^{+0.000}_{-443.756}$
$\sigma_{R_{\sigma\Lambda}} = 0.06$	$0.710^{+0.135}_{-0.173}$	$0.772^{+0.120}_{-0.159}$	$2.168^{+0.075}_{-0.186}$	$4.966^{+0.032}_{-0.475}$	$13.950^{+0.075}_{-1.423}$	$13.769^{+0.000}_{-1.064}$	$940.165^{+0.000}_{-430.676}$

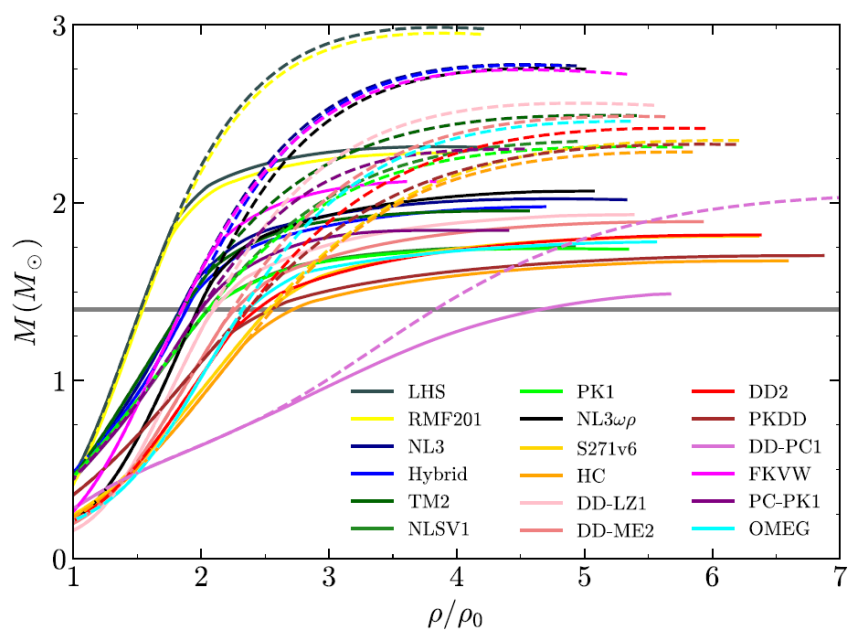
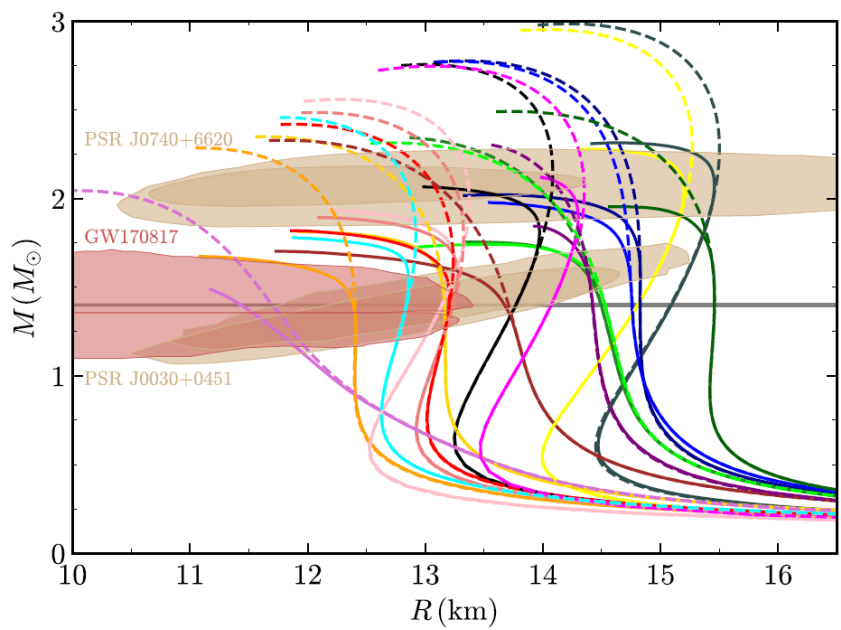
# Appendix



$$R_{\omega\Lambda} \approx \frac{-g_{\sigma N}\sigma}{U_N - g_{\sigma N}\sigma} R_{\sigma\Lambda} + \frac{U_\Lambda}{U_N - g_{\sigma N}\sigma}$$

$$R_{\omega\Lambda} \approx \frac{-\alpha_S^{NN} \rho_S}{U_N - \alpha_S^{NN} \rho_S - \beta_S^{NN} \rho_S^2 - \gamma_S^{NN} \rho_S^3 - \gamma_V^{NN} \rho_V^3 - \alpha_S^{N\Lambda} \rho_S^\Lambda - \alpha_V^{N\Lambda} \rho_V^\Lambda} R_{\sigma\Lambda} \\ + \frac{U_\Lambda}{U_N - \alpha_S^{NN} \rho_S - \beta_S^{NN} \rho_S^2 - \gamma_S^{NN} \rho_S^3 - \gamma_V^{NN} \rho_V^3 - \alpha_S^{N\Lambda} \rho_S^\Lambda - \alpha_V^{N\Lambda} \rho_V^\Lambda},$$

# Appendix



# Appendix

